Performance Analysis of a Shaded-Pole Linear Induction Motor Using Symmetrical Components, Field Analysis, and Finite Element Method

Innocent E. Davidson, *Member, IEEE,* and Jacek F. Gieras, *Senior Member, IEEE*

***Abstract*—The performance analysis of a shaded-pole linear induction motor using symmetrical components, field analysis and finite element methods is presented. Calculated results and measurements are compared and discussed.**

***Index Terms*—Field analysis, finite elements, linear induction motors, shaded-pole motors, symmetrical components.**

I. Shaded-Pole Motor

SHADED-POLE motors are recognized to be among one of the most robust and simple-to-design machines but difficult to analyze when compared to other induction motors [1].

The single-phase single-sided shaded-pole LIM with a rotating disc [2], and a stationary primary stack has salient poles with a main multiturn winding (phase a) with concentrated parameters and slots accommodating an auxiliary winding (shaded-pole) which is a single-turn shorted coil (phase b). Fig. 1 shows the construction of the shaded-pole LIM. It has a secondary consisting of a double-layer disc made of aluminum and back-iron plates. Table I shows the design data for the experimental machine.

Since the currents in the main and auxiliary windings are shifted by an angle less than $90°$ and the space angle between the two windings is also less than $90°$, an elliptical traveling magnetic field is produced in the airgap. The normal component of the magnetic flux density distribution in the airgap can be described by the following equation:

$$b(x,\,t) = \sum_{v=1}^{\infty} \left[B_{m\nu}^{+}\, e^{j(\omega_{s\nu}^{-} t - \beta_\nu x)} + B_{m\nu}^{-}\, e^{j(\omega_{s\nu}^{-} t + \beta_\nu x)} \right] \quad (1)$$

where $B_{m\nu}^{+}$ and $B_{m\nu}^{-}$ are the peak values of the νth space harmonic waves traveling in the x-direction (along the pole pitch), $\nu = 1,\, 3,\, 5 \cdots$ are the higher space harmonics, $\omega_{s\nu}^{+}$ is the angular frequency of the $s\nu$th harmonic of the forward~traveling field, $\omega_{s\nu}^{-}$ is the angular frequency of the $s\nu$th harmonic for the backward traveling field, $\beta_\nu = \nu\pi/\tau$, and τ is the pole pitch. The peak values of magnetic flux densities in (1) are:

$$B_{m\nu}^{+} = 0.5 \left[B_a b_{\nu a} + B_b b_{\nu b}\, e^{-j(\beta - \nu\alpha)} \right]$$

$$B_{m\nu}^{-} = 0.5 \left[B_a b_{\nu a} + B_b b_{\nu b}\, e^{-j(\beta + \nu\alpha)} \right]$$

Manuscript received April 22, 1998; revised February 1, 1999.

I. E. Davidson is with the Department of Electrical Engineering, Peninsula Technikon, Bellville 7535, South Africa (e-mail: IE_Davidson@yahoo.com).

J. F. Gieras is with United Technology Research Center, East Hartford, CT 06108 USA (e-mail: GierasJF@utrc.utc.com).

Publisher Item Identifier S 0885-8969(00)02208-7.

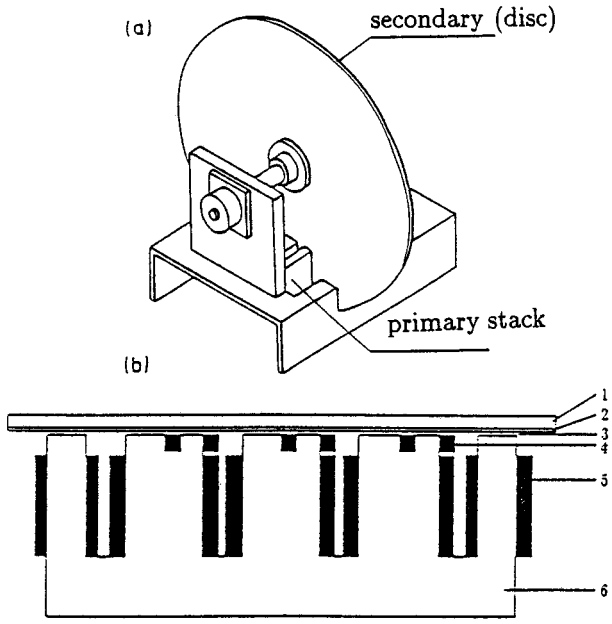

Fig. 1. Shaded-pole single-sided LIM: (a) general view and (b) longitudinal cross section. 1—secondary back iron, 2—aluminum cap, 3—airgap, 4—short-circuited coil, 5—main winding, and 6—primary stack.

where B_a is the normal component of the magnetic flux density (rectangular distribution) in the symmetry axis of the phase a and B_b is the normal components of the magnetic flux density (rectangular distribution) in the symmetry axis of the phase b, $b_{\nu a},\, b_{\nu b}$ are Fourier's coefficients, $\beta < 90°$ is the phase angle between the currents in phase a and b, and α is the angle between symmetry axes of phase a and b.

For $\nu = 1$ the angular frequencies with respect to the rotor are: $\omega_{s\nu=1}^{+} = 2\pi f s$, $\omega_{s\nu=1}^{-} = 2\pi f(2 - s)$ where s is the slip for fundamental harmonic. For further analysis, the fundamental space harmonic $\nu = 1$ will be assumed.

II. Symmetrical Components

In the circuital approach to the analysis of such a single-phase shaded-pole motor, symmetrical components for a 2-phase system are usually used. The rotating magnetic field remains circular under the following conditions:

a) The stator windings are spaced apart through an angle $\alpha = 90$ electrical degrees.
b) The currents through the stator windings are shifted in time by an angle $\beta = 90°$.

TABLE I
LIM DESIGN DATA

Quantity	Value	Unit
Length of primary stack	$L_\tau = 0.192$	m
Width of primary stack	$L_i = 0.09$	m
Number of pole pairs	$p = 2$	
Number of turns per main phase	$N_a = 520$	
Resistance of main winding for dc current	$R_{dc} = 12.813$	Ω
Primary winding factor	$k_{w1} = 1$	
Pole pitch	$\tau = 0.048$	m
Air gap	$g = 0.0015$	m
Height of pole	$h_P = 0.048$	m
Width of pole	$w_p = 0.016$	m
Diameter of wire with insulation	$d_w = 0.00125$	m
Cross sectional area of shading ring	1.227×10^{-6}	m^2
Height of shading ring slot	$h_s = 0.005$	m
Width of shading pole slot	$w_s = 0.005$	m
Diameter of disc	$d_{sec} = 0.52$	m
Thickness of ferromagnetic core	$h_{sec} = 0.010$	m
Thickness of Al layer	$d = 0.003$	m

c) The main and auxiliary windings are of equal MMF

$$I_b N_b k_{w,b} = I_a N_a K_{w,a} \tag{2}$$

where N is number of turns of the respective windings and k_w is winding factor. A shaded-pole induction motor does not meet the conditions a), b) and c).

Refer auxiliary winding to main stator winding side, $I'_b = I_b/k_{tr}$, where, $k_{tr} = N_a k_{w,a}/N_b k_{w,b}$, i.e., the transformation ratio of windings a and b, $k_{w,a}$, $k_{w,b}$ are winding factors, and N_a is the number of turns of the main winding.

From [2], the two-phase asymmetric system of vectors of currents $\dot{I}_a$ and $\dot{I}_b$ having unequal magnitudes and spaced apart by an arbitrary angle can be resolved into two symmetrical systems each composed of two vectors equal in magnitude and spaced $90°$ apart. The forward-sequence system of vectors is, $\dot{I}_a^+$ and $\dot{I}'^+_b$. It has the same phase sequence as the original system. The backward-sequence system of vectors is $\dot{I}_a^-$ and $\dot{I}'^-_b$.

Thus, for $\alpha = 90°$, $\dot{I}'^+_b = -j\dot{I}_a^+$ and $\dot{I}'^-_b = j\dot{I}_a^-$. For an angle $alpha \neq 90°$, the original and derived systems are equivalent hence, $\dot{I}_a^+ + \dot{I}_a^- = I_a$ and $\dot{I}'^+_b + \dot{I}'^-_b = I'_b$. Since the conditions a), b) and c) are not satisfied in the shaded-pole LIM, as spacing between a and b is not $90°$, $(\alpha < 90°)$, $I'_b \neq I_a$, hence the magnetic flux vector describes an ellipse.

The equation for current in the auxiliary winding (short-circuited coil) is:

$$I_b = j\left(\frac{I_a^+}{\sin\alpha} - \frac{I_a^-}{\sin\alpha}\right). \tag{3}$$

The input current in the main phase is

$$I_a = -j\left(\frac{I_a^+}{\sin\alpha}\, e^{j\alpha} - \frac{I_a^-}{\sin\alpha}\, e^{-j\alpha}\right). \tag{4}$$

III. EQUIVALENT CIRCUIT ANALYSIS

Separate equivalent circuits for two phases and for forward and backward sequences are set up to determine currents in the stator and rotor windings. The $+ve$ and $-ve$ sequence fields revolve at a different speed with respect to the rotor. This determines the expression for slip and impedances of the equivalent circuit. The equations for the main and auxiliary phases are:

- for the main winding

$$V_a = I_a Z_{1a} + I_a^+ Z^+ + I_a^- Z^- + (I_a + I_b) Z_{ab} \tag{5}$$

- for the auxiliary winding

$$V_b = 0 = I_b Z_{1b} + I_b^+ Z^+ + I_b^- Z^- + (I_a + I_b) Z_{ab} \tag{6}$$

where Z^+, Z^- are the $+ve$ and $-ve$ sequence impedances of the magnetization branch and secondary being in parallel.

For the positive sequence (forward traveling field), slip $s^+ = s$, and for the negative sequence (backward traveling field), slip $s^- = 2 - s$. The primary impedances in the equivalent circuit are:

$$Z_{1a} = R_{1a} + jX_{1a} \quad Z_{1b} = R_{1b} + jX_{1b} \tag{7}$$

for the main and auxiliary windings, respectively. In the above equations, R_{1a}, X_{1a} is the resistance and leakage reactance of the main phase of stator winding. For the magnetization branch of the equivalent circuit,

$$Z_o = R_o + jX_o = \frac{R_{\mathrm{Fe}} X_m^2}{R_{\mathrm{Fe}}^2 + X_m^2} + j\,\frac{R_{\mathrm{Fe}}^2 X_m}{R_{\mathrm{Fe}}^2 + X_m^2} \tag{8}$$

where R_{Fe} is the resistance representing core losses and X_m is the mutual reactance between primary and secondary circuit. There is also an additional impedance in series with the primary impedance, i.e.,

$$Z_{ab} = jX_{ab} = j\omega M_{ab} \tag{9}$$

where X_{ab} is mutual reactance between main phase a and auxiliary phase b. In practical calculations,

$$X_{ab} \approx \frac{\alpha_b}{\alpha_a}\,\frac{Z_o}{2p}$$

where α_b is the angle corresponding to the width of shading ring and α_a is the angle corresponding to the width of the main pole. The secondary impedance Z'_2 is discussed in Section IV. Fig. 2 shows the equivalent circuit of the shaded-pole motor for the positive and negative sequences for phases a and b.

IV. ROTOR (SECONDARY) IMPEDANCE

The impedances of the aluminum cap and the solid back iron the fundamental space harmonic $\nu = 1$ are [3],

$$Z'_{\mathrm{Al}}(s) = \frac{js\omega\mu_0}{k_{\mathrm{Al}}}\,\frac{1}{\tanh(k_{\mathrm{Al}}\, d)}\, k_{\mathrm{tr}}\frac{L_i}{\tau} \tag{10}$$

$$Z'_{\mathrm{Fe}}(s) = \frac{js\omega\mu_{\mathrm{Fe}}}{k_{\mathrm{Fe}}}\,\frac{1}{\tanh(k_{\mathrm{Fe}} h_{sec})}\, k_{\mathrm{tr}} k_z\,\frac{L_i}{\tau} \tag{11}$$

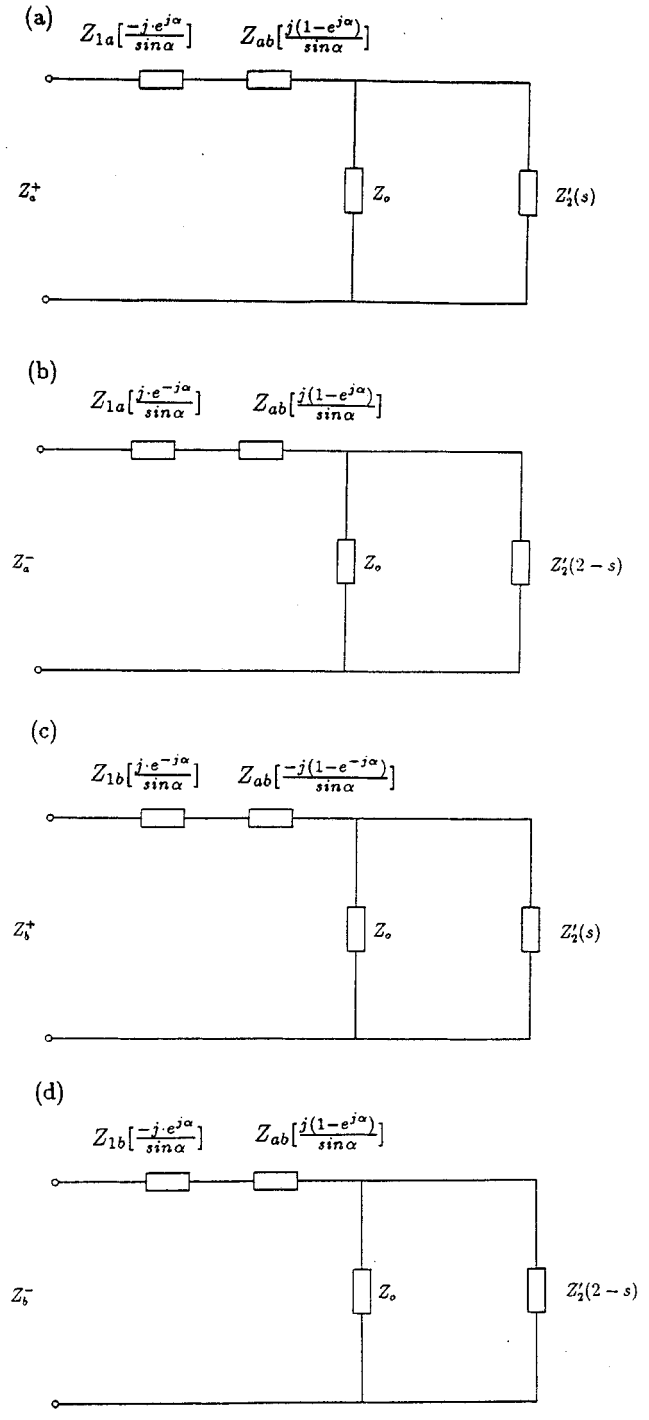

Fig. 2. Equivalent circuits of a shaded pole induction motor: (a) phase a, positive sequence, (b) phase a, negative sequence, (c) phase b, positive sequence, and (d) phase b, negative sequence.

where the propagation constant for aluminum is

$$k_{\mathrm{Al}} = \sqrt{js\omega\mu_0\sigma'_{\mathrm{Al}} + \left(\frac{\pi}{\tau}\right)^2} \tag{12}$$

and the propagation constant for iron is

$$k_{\mathrm{Fe}} = \sqrt{js\omega\mu_{\mathrm{Fe}}\sigma_{\mathrm{Fe}} + \left(\frac{\pi}{\tau}\right)^2}. \tag{13}$$

The coefficient including transverse edge effect in aluminum layer, k_{rn} for fundamental, is [5]

$$k_{rn} = 1 - \frac{\tanh\left(\beta\,\frac{w}{2}\right)}{\beta\,\frac{w}{2}\,\left(1+\tanh\left(\beta\,\frac{w}{2}\right)\tanh\left(\beta h_{ov}\right)\right)} \tag{14}$$

where $\beta = \pi/\tau$, the effective width of the secondary ferromagnetic core $w = \tau + L_i$, L_i is the effective width of the primary core, and h_{ov} is the secondary winding overhang.

Equivalent conductivity of aluminum cap including the transverse edge effect is

$$\sigma'_{\mathrm{Al}} = k_{rn} \times \sigma_{\mathrm{Al}}$$

where σ_{Al} is the conductivity of aluminum.

The transverse edge effect coefficient for the back iron is given by the equation [5],

$$k_z = 1 - \frac{g}{L_i} + \frac{2}{\pi}\,\frac{\tau}{w}\,\left[1-\exp\left(-\frac{\pi}{2}\,\frac{w}{L_i}\right)\right]. \tag{15}$$

Equations (10) and (11) apply to the forward sequence slip s. For the backward sequence slip $2-s$,

$$Z'_{\mathrm{Al}}(2-s) = \frac{j(2-s)\omega\mu_o}{k_{\mathrm{Al}}}\,\frac{1}{\tanh(k_{\mathrm{Al}}\,d)}\,k_{\mathrm{tr}}\,\frac{L_i}{\tau} \tag{16}$$

$$Z'_{\mathrm{Fe}}(2-s) = \frac{j(2-s)\omega\mu_{\mathrm{Fe}}}{k_{\mathrm{Fe}}}\,\frac{1}{\tanh(k_{\mathrm{Fe}}h_{sec})}\,k_{\mathrm{tr}}k_z\,\frac{L_i}{\tau} \tag{17}$$

where

$$k_{\mathrm{Al}} = \sqrt{j(2-s)\omega\mu_0\sigma'_{\mathrm{Al}} + \left(\frac{\pi}{\tau}\right)^2} \tag{18}$$

$$k_{\mathrm{Fe}} = \sqrt{j(2-s)\omega\mu_{\mathrm{Fe}}\sigma_{\mathrm{Fe}} + \left(\frac{\pi}{\tau}\right)^2}. \tag{19}$$

Thus, the secondary impedances referred to the primary system of a single-sided LIM for the fundamental harmonic and the induced voltage across the magnetization branch independent of the slip is,

$$Z'^{+}_{2} = Z'_2(s) = \frac{Z'_{\mathrm{Al}}(s)Z'_{\mathrm{Fe}}(s)}{Z'_{\mathrm{Al}}(s)+Z'_{\mathrm{Fe}}(s)}\,\frac{1}{s} = \frac{R'_2(s)}{s} + j\,\frac{X'_2(s)}{s} \tag{20}$$

$$Z'^{-}_{2} = Z'_2(2-s) = \frac{Z'_{\mathrm{Al}}(2-s)Z'_{\mathrm{Fe}}(2-s)}{Z'_{\mathrm{Al}}(2-s)+Z'_{\mathrm{Fe}}(2-s)}\,\frac{1}{2-s}. \tag{21}$$

Total impedance as seen from the input terminals of the equivalent circuit,

$$Z_t^+ = j\,\frac{Z_{1a}\cdot e^{j\alpha}}{\sin\alpha} - j\,\frac{Z_{ab}(1-e^{j\alpha})}{\sin\alpha} + Z^+ \tag{22}$$

$$Z_t^- = j\,\frac{Z_{1a}\cdot e^{-j\alpha}}{\sin\alpha} - j\,\frac{Z_{ab}(1-e^{-j\alpha})}{\sin\alpha} + Z^-. \tag{23}$$

The impedances of the magnetization and secondary branch in parallel are

$$Z^+ = \frac{Z_0\cdot Z'^{+}_{2}}{Z_0+Z'^{+}_{2}} \quad Z^- = \frac{Z_0\cdot Z'^{-}_{2}}{Z_0+Z'^{-}_{2}}. \tag{24}$$

If the core losses are negligible ($R_{\rm Fe} = 0$), then

$$Z^+ \approx \frac{jX_m Z'^+_2}{Z'^+_2 + jX_m} \quad Z^- \approx \frac{jX_m Z'^-_2}{Z'^-_2 + jX_m}. \tag{25}$$

V. Calculation of Currents

To obtain expressions for the positive and negative sequence main phase currents in terms of $V,\ \alpha,\ Z_{1a}, Z_{1b},\ Z^+,\ Z^-$, recall (3) and (4) for I_a and I_b, and substituting in (5) and (6), respectively, gives;

$$I_a^+ = \frac{V_a\left[Z_{1b} + Z_{ab}(1 - e^{-j\alpha}) + jZ^- e^{-j\alpha}\sin\alpha\right]}{\sin\alpha[G1 + G2]} \tag{26}$$

and

$$I_a^- = \frac{V_a\left[Z_{1b} + Z_{ab}(1 - e^{j\alpha}) - jZ^+ e^{j\alpha}\sin\alpha\right]}{\sin\alpha[G1 + G2]} \tag{27}$$

where

$$G1 = (Z_{1a} + Z_{1b})\,(Z^+ + Z^- + 2Z_{ab})$$

$$G2 = 2\left[Z_{1a}Z_{1b} + Z^+Z^-\sin^2\alpha + Z_{ab}(Z^+ + Z^-)\,(1 - \cos\alpha)\right].$$

The symmetrical components of the secondary currents referred to the main winding as obtained from the equivalent circuits are

$$I'^+_2 = I_a^+\,\frac{|Z_o|}{|Z_o + Z'^+_2|} \tag{28}$$

$$I'^-_2 = I_a^-\,\frac{|Z_o|}{|Z_o + Z'^-_2|} \tag{29}$$

where Z'^+_2 and Z'^-_2 are forward and backward impedances of the secondary referred to the main stator winding turns according to (20) and (21).

VI. Electromagnetic Torque

The electromagnetic torque components for the forward and backward sequence are,

$$T^+ = \frac{2(I'^+_2)^2 R'_2(s)}{\omega_1 s} \tag{30}$$

$$T^- = \frac{2(I'^-_2)^2 R'_2(2-s)}{\omega_1(2-s)} \tag{31}$$

where I'^+_2, I'^-_2 are the secondary currents referred to the stator main winding, and R'^+_2, R'^-_2 are the referred rotor resistances. These components are referred to the secondary side by the transformation factor between the stator and rotor of motor, $k = 2m(N_a k_{w,a})^2/p$. The difference between the positive and negative sequence torques is the resultant torque $T = T^+ - T^-$.

VII. Analysis of Electromagnetic Field

The general solutions of equations for electromagnetic field distribution in a salient pole induction machine, gives the following recurrence relations [6], [7]. For $0 \le z \le d_k$,

$$H_{zk}^{(k)} = \sum_{\nu=1}^{\infty}\sum_{n=1}^{\infty}\frac{1}{M_k^{(k)}}\left[\frac{1}{\chi_k}H_{zk-1}^{(k-1)}(x,\,y,\,0)\times\cosh\chi_k(z-d_k) + \frac{1}{j\omega_{k-1}\mu_{k-1}}\frac{\mu_{k-1}}{\mu_k}\times E_{yk-1}^{k-1}(x,\,y,\,0)\sinh\chi_k(z-d_k)\right]\times\frac{\mu_1}{\mu_k}\frac{\chi_k}{\chi_1}H_{xl}^{(1)} \tag{32}$$

$$H_{zk}^{(k)} = \sum_{\nu=1}^{\infty}\sum_{n=1}^{\infty}\frac{1}{M_k^{(k)}}\left\{\frac{1}{\chi_k}\left[-H_{zk-1}^{(k-1)}(x,\,y,\,0)\right]\times\sinh\chi_k(z-d_k) + \frac{1}{j\omega_k\mu_{k-1}}\frac{\mu_{k-1}}{\mu_k}\times\left[-E_{yk-1}^{k-1}(x,\,y,\,0)\right]\times\cosh\chi_k(z-d_k)\right\}\times\frac{\mu_1}{\mu_k}H_{z1}^{(1)} \tag{33}$$

$$E_{yk}^{(k)} = \sum_{\nu=1}^{\infty}\sum_{n=1}^{\infty}\frac{1}{M_k^{(k)}}\left\{\frac{1}{\chi_k}\left[-H_{zk-1}^{(k-1)}(x,\,y,\,0)\right]\times\sinh\chi_k(z-d_k) + \frac{1}{j\omega_{k-1}\mu_{k-1}}\frac{\mu_{k-1}}{\mu_k}\left[-E_{yk-1}^{k-1}(x,\,y,\,0)\right]\cosh\chi_k(z-d_k)\right\}\times\frac{\omega_k}{\omega_1}E_{y1}^{(1)}. \tag{34}$$

For the fundamental harmonic, ν = 1, equations were obtained for the respective layers for i = 1, 2, 3 and 4, where 1—air halfspace, 2—back iron, 3—aluminum, and 4—airgap. For the shaded-pole LIM, these equations were used to solve for $\boldsymbol{B}$, and to calculate the normal and tangential forces, and hence torque using the field approach. The forces acting on the secondary are given by:

$$F_x = -\frac{1}{2\mu_0}\Re\left[\boldsymbol{B}_y\boldsymbol{B}_x^*\right](2p\tau L_i) \tag{35}$$

$$F_y = \frac{1}{2\mu_0}\Re\left[\frac{1}{2}\boldsymbol{B}_{my}\boldsymbol{B}_{my}^* - \frac{1}{2}\boldsymbol{B}_{mx}\boldsymbol{B}_{mx}^*\right](2p\tau L_i) \tag{36}$$

where μ_0 is the magnetic permeability of free space, $\boldsymbol{B}_y$, $\boldsymbol{B}_x$ are the normal and tangential components of magnetic flux density in the airgap, and L_i is the effective length of the primary stack (in the z-direction). The shaft torque is obtained from the expression, $T = F_x r$, where r is the radius of disc.

VIII. Finite Element Analysis

The 2-D electrodynamic field distribution is described by the following differential equations:

- for the primary windings:

$$\frac{\partial}{\partial x}\left(\frac{1}{\mu}\frac{\partial \boldsymbol{A}}{\partial x}\right) + \frac{\partial}{\partial y}\left(\frac{1}{\mu}\frac{\partial \boldsymbol{A}}{\partial y}\right) = -\boldsymbol{J}_z(x,\,y) \tag{37}$$

- for the disc rotor:

$$\frac{\partial}{\partial x}\left(\frac{1}{\mu}\frac{\partial \boldsymbol{A}}{\partial x}\right)+\frac{\partial}{\partial y}\left(\frac{1}{\mu}\frac{\partial \boldsymbol{A}}{\partial y}\right)-\sigma v\frac{\partial \boldsymbol{A}}{\partial x}=j\omega\sigma \boldsymbol{A}_{mz} \quad (38)$$

where $\boldsymbol{A}$ is the magnetic vector potential, $\boldsymbol{J}$ is the current density, σ is the electric conductivity, v is the linear speed of rotor, and $\mu=\mu_0\mu_r$ is the magnetic permeability. The x-coordinate is in the direction of motion, the y-coordinate is perpendicular to the active surfaces, and the z-coordinate is in the radial direction. The following assumptions have been made in the FEM analysis:

a) LIM has finite dimensions along the x (pole pitch) and y (normal) directions but infinitely long in the z-direction (end effects are neglected).
b) The relative motion of the LIM secondary is assumed to be in the x-direction only, and all currents are constrained to flow in the z-direction only.
c) The magnetic permeability of the primary stack and secondary back iron is a nonlinear function of the magnetic field intensity.

The magnetic field distribution in the longitudinal section of the LIM using Infolytica Magnet 5 FEM package is shown in Fig. 3. The force in the x-direction acting on the rotating disc has been calculated using the FEM and Maxwell's stress tensor method. The forces acting on the secondary are given by the following equations:

$$F_x=\frac{L_i}{\mu_0}\int B_y B_x\, dl \quad (39)$$

$$F_y=\frac{L_i}{2\mu_0}\int \left[B_y^2-B_x^2\right]\, dl \quad (40)$$

where μ_0 is the magnetic permeability of free space, $\boldsymbol{B}_y$, $\boldsymbol{B}_x$ are the normal and tangential components of magnetic flux density in the airgap, and L_i is the effective length of the primary stack (in the z-direction). The normal and tangential force components are thus calculated and shaft torque obtained from the expression, $T=F_x r$, where r is the radius of disc.

IX. Comparison of Results

The steady-state load characteristics, i.e., thrust and normal force versus speed at different power frequencies have been calculated using the symmetrical components, field theory approach, and FEM. These calculated results were compared with experimental tests performed on the shaded-pole LIM using sinusoidal excitation at varying power frequencies from 50–75 Hz. Symmetrical components gave the best performance prediction. The 2-D FEM is versatile in the computation of field parameters especially for magnetostatic analysis. The field approach is not flexible in modeling the LIM, hence results show much deviation with varying frequency.

Figs. 4–6 show the shaft torque $T=F_x r$ against velocity at constant frequency. The variation of measured efficiency with increasing frequency is shown in Fig. 7. With a large airgap of 1.5 mm, the magnetizing current in the LIM increases significantly and consequently the input rms current and stator I^2R loss in the shading coil, thereby reducing the efficiency and power factor $\cos\varphi$. The efficiency of the investigated LIM

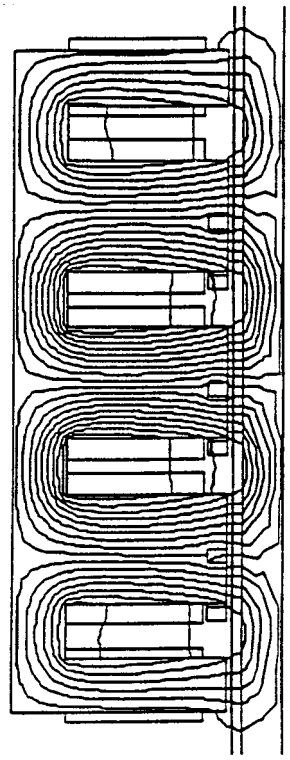

Fig. 3. Magnetic field distribution in the longitudinal section of the LIM.

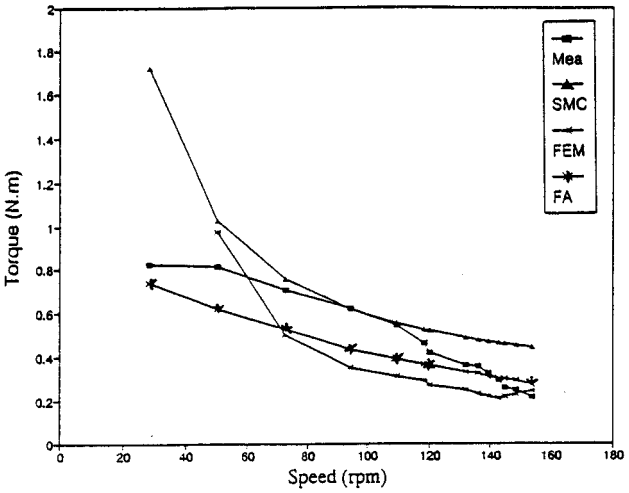

Fig. 4. Torque against linear velocity at f = 75 Hz.

is low. The influence of edge effects is minimal in low speed LIM's. However, saturation effects and the presence of third time harmonics in the voltage and current waveforms contribute to errors in calculations, so that the error in calculations are higher than in high performance machines. From tests, it was observed that increasing frequency of supply gives better mechanical performance such as: less vibrations, improved torque and efficiency.

X. Conclusions

The application of symmetrical components of two-phase asymmetric systems, field theory, and FEM to the performance

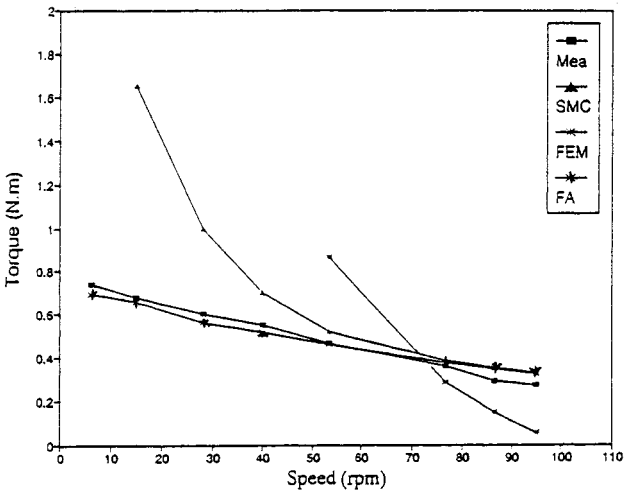

Fig. 5. Torque against linear velocity at f = 60 Hz.

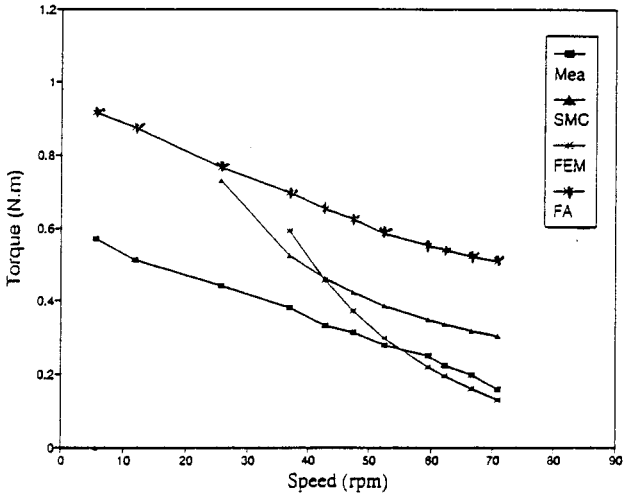

Fig. 6. Torque against linear velocity at f = 50 Hz.

calculation of the shaded-pole LIM has been presented. The results compared with measurements are satisfactory though the performance of the shaded-pole single-phase LIM is poor when compared to three-phase LIM's. LIM's generally have low efficiencies due to their open airgap. The maximum efficiency of rotary shaded-pole induction motors with cage-rotors rated

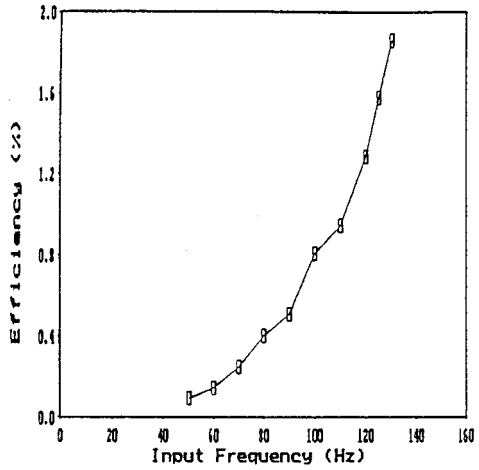

Fig. 7. Efficiency versus input frequency.

at 100 W usually does not exceed 20%. The efficiency of the shaded-pole LIM is very low at power frequency. However, it has been found that the efficiency can be improved by reducing voltage and increasing the input frequency.

The shaded-pole LIM can find applications in turntables used in industry or in small mechanisms where a three-phase power supply is not available and low torque is acceptable or where the price and simplicity of the drive is important.

REFERENCES

[1] M. Akbaba and S. Q. Fakhro, "Field distribution and iron loss computation in reluctance augmented shaded-pole motors using finite element method," *IEEE Trans. on Energy Conversion*, vol. 7, no. 2, pp. 302–307, 1992.

[2] I. E. Davidson, "Performance calculation for a single-phase single-sided shaded-pole linear induction motor using symmetrical components and finite element method," *Electromotion Journal*, vol. 4, no. 4, 1997.

[3] J. F. Gieras, *Linear Induction Drives.* Oxford: Clarendon Press, 1994.

[4] M. Akbaba and S. Q. Fakhro, "An improved computational technique of the inductance parameters of reluctance augmented shaded-pole motors using finite element method," *IEEE Trans. on Energy Conversion*, vol. 7, no. 2, pp. 308–314, 1992.

[5] J. F. Gieras, "Calculation of resistances and reactances of a single-sided linear induction motor," *ETEP*, vol. 2, no. 6, 1992.

[6] I. Boldea and M. Babescu, "Multilayer approach to the analysis of single sided linear induction motors," *IEEE Proc.*, vol. 125, no. 4, pp. 283–287, Apr. 1978.

[7] J. F. Gieras, "Analysis of multilayer rotor induction motor with higher space harmonies taken into account," *IEE Proc.*, pt. B, vol. 138, pp. 32–36, 1991.